Calculation of Soret-Shifted Dew Points by Continuous Mixture Thermodynamics

Daniel E. Rosner, Manuel Arias-Zugasti, and Barbara LaMantia
High Temperature Chemical Reaction Engineering Laboratory and Yale Center for Combustion Studies, Dept. of Chemical Engineering, Yale University, New Haven, CT 06520

DOI 10.1002/aic.10515
Published online June 30, 2005 in Wiley InterScience (www.interscience.wiley.com).

Soret-induced local concentration changes, very large numbers of condensable species, and condensate nonideality combine to make the calculation of isobaric dew-point surface temperatures, T_{dp}, and corresponding incipient condensate compositions (x_i, $i = 1, 2, \ldots, N$) nontrivial, even with advanced computational methods. As usual in the canonical isobaric "dew-point " situation, the mainstream vapor mixture state [composition y_i ($i = 1, 2, \ldots, N$), T, and p] is fully specified. We consider here, for illustrative purposes, the tractable but frequently encountered limiting case of a very large number (perhaps dozens, if not hundreds) of condensable, nonreacting species that are members of a homologous series (such as n-alkanes in a fuel "blend"), dilute in a "noncondensable " carrier gas (such as N_2). Pseudo-binary Ludwig–Soret coefficients for the vapor phase are estimated from the corresponding Schmidt numbers and gas-kinetic theory. As in our earlier studies (which emphasized binary "regular " solutions of alkali sulfates), of particular current interest is the extent of systematic Soret-induced shifts in the predicted dew-point (wall) temperature and associated condensate composition/properties (such as viscosity). This often-overlooked feature removes the present class of univariate problems from the province of classical continuous thermodynamics. Three efficient continuous mixture theory (CMT)–based computational methods are proposed/illustrated/compared, two moment-based, and all exploiting Gaussian quadratures. We find that accurate results can be obtained while avoiding prescribing the shape of the distribution function in the condensate, using as few as three to four rationally selected "pseudo-components." © 2005 American Institute of Chemical Engineers *AIChE J,* 51: 2811–2824, 2005
Keywords: continuous mixture theory, Ludwig-Soret transport, quadrature method of moments, orthogonal colocation, nonideal mixtures

Introduction

Motivation, background, and objectives

Dew-point loci on phase diagrams are usually thought of as purely thermodynamically dictated. However, even when the conditions of phase equilibria are locally valid at, say, a gas mixture/condensed phase boundary, the conditions there are frequently systematically different from those established in the mainstream or feed. Such differences can be caused by several phenomena, but one mechanism frequently encountered in high-temperature multicomponent systems is Ludwig–Soret (L-S) species mass transport.[1,2] Put simply, when there is a steady-state temperature gradient established in the vicinity of such an interface, then, at incipient condensation, the condition of zero species (or element) flux necessarily implies the presence of nonzero composition gradients normal to the interface. Thus, the combination of temperature and species composition established *at* such an interface can be quite

M. Arias-Zugasti is also affiliated with Depto. de Física Matemática y Fluidos, Facultad de Ciencias UNED, Apdo. 60141, 28080 Madrid, Spain.
Correspondence concerning this article should be addressed to D. E. Rosner at daniel.rosner@yale.edu.

different from that set (perhaps by the experimenter) in the mainstream or feed.

Our previous laboratory and theoretical studies of high-temperature dew points in combustion systems containing condensable vapors were focused on corrosive alkali sulfates, with emphasis on the formation of binary nonideal liquid solutions such as $Na_2SO_4 + K_2SO_4$ (see, for example, Rosner and Liang[3] and Liang and Rosner[4]). In the present paper we return to this canonical problem, generalizing our procedures to now embrace a mainstream that contains a family of condensable species, each member of which is influenced by the temperature gradient prevailing near the actively cooled solid surface, that is, the site of multicomponent condensation if the temperature falls below the (Ludwig–Soret-shifted) dew point. Indeed, for illustrative purposes we explicitly consider below a mainstream mixture of *n*-alkane fuel vapors dilute in a N_2(g) carrier gas flow. When the number of individual condensable species (N) is large enough [usually $N \gtrsim O(10)$], we exploit the attractive formalism of *continuous mixture theory* (CMT: see, for example, Gal-Or et al.[5] and Cotterman and Prausnitz[6] and the references cited therein) to facilitate such engineering calculations (of T_{dp} and the associated condensate composition, x_i, $i = 1, 2, \ldots, N \gg 1$). We note that, in the present (not atypical) cases, whereas nonideality may be neglected in the vapor phase, nonideality must be dealt with in the condensate phase (here because of the broad spectrum of molecular aspect ratios considered). Thus, with the aid of this model problem, we can simultaneously illustrate the effects on T_{dp} and x_i of the following:

(1) L-S–modified compositions in the immediate vicinity of the condensation site.

(2) Alternate CMT solution algorithms, including two attractive numerical solution methods (*quadrature method of moments* and *spectral orthogonal collocation*, hereafter abbreviated QMOM and SOC) that do not presume the shape of the probability density function (PDF) in the condensate.

(3) The role of modest solution nonideality in modifying predicted dew points, PDF shapes, and associated condensate properties (such as viscosity).

(4) Validity of the continuous mixture representation of even fuel mixtures of modest complexity (containing as few as 12 real species).

As a safety-related by-product, we also show how the present CMT formulation lends itself to rational predictions of the lower flammability limit (LFL) of the vapor mixture established adjacent to the surface, presuming, of course, the presence of air (not pure N_2) as the carrier gas, and also the existence of an ignition source of adequate energy/duration.

In the next section we summarize our CMT reformulation of the canonical dew-point problem, including our sources/treatment of input transport and thermodynamic data for *n*-alkane mixtures. Three basic solution methods will be described/illustrated, including two moment-based methods: the usual *method of moments* (MOM), based in a "presumed mathematical form" PDF for the condensate composition; and the quadrature method of moments (QMOM), which has the merit that it does not presume the shape of the PDF in the condensate phase. We also illustrate the use of a spectral orthogonal collocation method (SOC), which similarly to the QMOM does not presume the shape of the PDF of the condensate, and which will be particularly convenient for a broad class of such CMT problems, including multicomponent, multiphase rate problems (such as liquid fuel blend evaporation, with or without vapor-phase combustion[7]). Our numerical results for the present class of transport-shifted dew-point problems, including all of the above-mentioned instructive comparisons, are presented in the following section. The final section then summarizes our broader conclusions and recommendations.

Continuous-Mixture Formulation of the Canonical Dew-Point Problem

Basic assumptions of the present nonequilibrium thermodynamics model

The following simplifying assumptions underlie our present formulation/illustrative numerical calculations:

A1. No chemical transformations occur either in the vapor phase, at the vapor/liquid interface itself, or in the (incipient) condensate phase. As a corollary, the upper and lower molecular weight (MW) cutoffs (used to represent the fuel blends) apply in both phases.

A2. Steady-state, isobaric, pseudo-binary molecular transport in the absence of a net species flux to/from the liquid/vapor interface.

A3. Local vapor/liquid equilibrium (VLE) for each molecular species present in both phases.

A4. Carrier gas (N_2) sparingly soluble in the *n*-alkane condensate mixture at the prevailing composition, total pressure, and calculated dew-point temperature.

A5. The *n*-alkane fuel blends considered here (representing gasoline, diesel fuel, and aviation JP4 fuel with respect to nominal volatility) contain a sufficient number of chemical constituents to be considered a "continuous mixture," using carbon number (n in the formula C_nH_{2n+2}) or its MW counterpart, as the relevant "state" variable.

A6. Although the *vapor* phase may be considered thermodynamically ideal, the condensate will be nonideal, with modest negative deviations from Raoult's law associated with the spectrum of *n*-alkanes present.

A7. There is no appreciable barrier to, or facilitator of, heterogeneous nucleation—that is, phase change on the "cold" test surface occurs under thermodynamic "saturation" conditions.

A8. Continuity of temperature at the vapor/liquid interface, despite the presence of a nonzero energy flux (directed toward the condensate).

It is interesting to remark that A1 precludes the chemical vapor deposition (CVD) reactions that characterized our previous work on alkali–sulfate formation from simpler vapor precursors (such as NaOH, Na, SO_2, etc.) in the combustion gases.[2,8] A2 exploits the diluteness of the mainstream *n*-alkane + N_2 mixture—allowing us to invoke previously determined Soret factors for each of these *n*-alkanes when present in a background gas of N_2 (or air).[9,10] Of the assumptions itemized above, we will most carefully examine A5—that is, success of the "continuous mixture" representation. We will find that the CMT representation is more than adequate for the case of diesel fuel (21 discrete species; see below) and, perhaps, marginal for our 12-component representation of JP4. Condensate nonideality (A6), although systematically incorporated here by our UNIFAC evaluation of the relevant component activity coefficients (see, for example, Poling et al.[11]), will be found to

be modest in the present cases, being dominated by the much larger effects of carbon number on the vapor-phase Soret coefficients.[10] A7 emphasizes that we are dealing here with quasi-planar-phase boundaries, without the need to invoke local supersaturations or undersaturations associated with the now-familiar Gibbs–Kelvin effect. Finally, A8, included for completeness, precludes a significant interfacial temperature "jump" associated with the net energy flux—that is, we assume that the vapor temperature evaluated at the vapor/liquid interface is not significantly higher than the local liquid condensate temperature (see, for example, Rosner and Papadopoulos[12]). Under our present (atmospheric pressure, modest temperature) conditions, such temperature jumps would be insignificant compared to the predicted Soret-induced dew-point temperature shifts (here about 13 K). In the last section, dealing with generalizations/future work, we will briefly return to several of these assumptions. With this background we are now in a position to express this idealized physical model as a mathematical model—setting forth the governing equations that will allow us to numerically find the Soret-shifted dew-point temperature and associated condensate composition consistent with the imposed *n*-alkane mixture + N_2 "mainstream."

Incipient condensation phase equilibrium condition

We imagine a situation realized for many "dew-point" instruments—that is, consider immersing a temperature-controlled smooth surface into a slowly flowing multicomponent vapor mixture under nearly isobaric conditions. If this surface is gradually cooled to successively lower temperatures, we ask: at what temperature would condensation begin, and what would be the chemical composition of the "incipient condensate"? In the case of a discrete number (N) of condensable species present in a noncondensable carrier gas, we will completely specify the state of the mainstream mixture by its composition (y_∞^i, $i = 1, 2, \ldots, N$), temperature (T_∞), and pressure (p). As discussed below, just before condensation we have a situation in which there is zero flux of each species to/from the surface, but there is a steady-state temperature gradient explained by the fact that $T_{dp} < T_\infty$. In general this means that we cannot assume that the species concentrations established at the surface (y_w^i) are equal to the specified mainstream values (y_∞^i). Nevertheless, we usually can assume (see A3 above) that VLE is achieved at the incipient vapor/liquid-phase boundary, allowing us to write

$$\gamma_i(T_{dp})\, x_i p_i^{sat}(T_{dp}) = y_{i,w} p \qquad i = 1, 2, \ldots, N \tag{1}$$

where the γ_i are the liquid phase activity coefficients, dependent on both (as yet unknown) liquid-phase chemical composition and the dew-point temperature T_{dp}. Considering that the solubility of the carrier gas is negligible, the normalization condition of the condensate mole fractions

$$\sum_{i=1}^{N} x_i = 1 \tag{2}$$

closes the former system for the condensate composition and dew-point temperature. Because we are interested in situations containing a large number (usually $\gg 10$) of closely related condensable species, in the present case *n*-alkane fuel species within the "cutoff" interval $n_{\min} \le n \le n_{\max}$, it becomes attractive to pass to the continuous limit. Explicitly working with the carbon number n (for the general *n*-alkane C_nH_{2n+2}), the VLE condition Eq. 1 above becomes

$$\gamma(n, T_{dp})\, x(n)\, p^{sat}(n, T_{dp}) = y_w(n)\, p \qquad n \in [n_{\min}, n_{\max}] \tag{3}$$

and the normalization condition Eq. 2 becomes

$$\frac{N}{N-1} \int_{n_{\min}}^{n_{\max}} x(n)\, dn = 1 \tag{4}$$

where the normalization factor $N/(N-1)$, a number close to 1, is a consequence of the finite upper cutoff $n_{\max}$.

Before moving on we should comment on the incentive to pass to the "continuous mixture" limit. At first glance it might seem strange to replace a well-posed problem involving N discrete species by one with an "infinite" number (continuum) of species! However, as will be seen, using the CMT reformulation it is possible to obtain accurate solutions to such problems with the rational choice of a much smaller number ($\hat{N}$), often only 3 or 4, of "pseudo-species," explicitly or implicitly found from the roots of a polynomial on the domain [$n_{\min}$, $n_{\max}$].

Ludwig–Soret "enrichments" in the vicinity of the condensation surface

As a consequence of the Ludwig–Soret transport, the total fuel vapor mole fraction established at the vapor/liquid interface (y_w^F) is systematically different from the specified value y_∞^F in the mainstream. We will find that the vapor-phase PDF $y_w(n)$, appearing in Eq. 3, is readily calculated from the specified $y_\infty(n)$ by taking into account the Ludwig–Soret-induced species segregation that occurs across the inevitable thermal boundary layer.

In the present case the zero molecular species flux condition is satisfied when the L-S flux of fuel species i toward the "cold" surface is balanced by the outgoing Fick-flux of species i.[9] In the dilute, isobaric, pseudo-binary limit, this leads to the conclusion that

$$\frac{y_{i,w}}{y_{i,\infty}} = \left(\frac{T_\infty}{T_{dp}}\right)^{\alpha_i^T} \qquad i = 1, \ldots, N \tag{5}$$

where α_i^T is the appropriate mean[1] thermal diffusion factor for species i in the N_2 background gas.[9,10] As a corollary of Eq. 5 above, we find the following interesting explicit result for the steady-state PDF $y_w(n)$

$$y_w(n) = y_\infty(n) \left(\frac{T_\infty}{T_{dp}}\right)^{\alpha_T(n)} \qquad n_{\min} \le n \le n_{\max} \tag{6}$$

[1] Because α_i^T is slightly T-dependent, in the present cases we evaluated α_i^T at the mean boundary layer (BL) temperature: $T_{BL} \equiv \frac{T_{dp} T_\infty}{T_{dp} - T_\infty} \ell n \frac{T_{db}}{T_\infty}$.

which must be used in the CMT version of the VLE condition Eq. 3 above. It also follows that

$$\frac{y_{F,w}}{y_{F,\infty}} = \frac{N}{N-1}\int_{n_{\min}}^{n_{\max}} \frac{y_\infty(n)}{y_{F,\infty}}\left(\frac{T_\infty}{T_{dp}}\right)^{\alpha_T(n)} dn \tag{7}$$

corresponding to a slight reduction in steady-state N_2 mole fraction established at the condensate surface.

Treatment of solution nonideality

To show that the present CMT methods can be used under rather general conditions, the activity coefficients of the (slightly) nonideal liquid mixture have been computed here according to the UNIFAC method.[11,13] Thus, each activity coefficient is given by a *combinatorial* part (γ_i^C) times a *residual* part (γ_i^R)

$$\ln \gamma_i = \ln \gamma_i^C + \ln \gamma_i^R \tag{8}$$

where the *combinatorial* part has been computed by the UNIFAC method, as a function of the pure component *areas* q_i and *volumes* r_i, according to

$$\ln \gamma_i^C = \ln \frac{\Phi_i}{x_i} + \frac{z}{2} q_i \ln \frac{\theta_i}{\Phi_i} + l_i - \frac{\Phi_i}{x_i}\sum_{j=1}^{N} x_j l_j \tag{9}$$

where

$$\Phi_i = \frac{x_i r_i}{\sum_{j=1}^{N} x_j r_j} \qquad \theta_i = \frac{x_i q_i}{\sum_{j=1}^{N} x_j q_j}$$

$$l_i = \frac{z}{2}(r_i - q_i) - (r_i - 1) \tag{10}$$

where z is the coordination number, which has been taken as $z = 10$. In the former equation the pure component parameters r_i and q_i have been calculated as the sum of the group *volumes* (R_i) and *areas* (Q_i) corresponding to each group present in the component i

$$r_i = \sum_{j=1}^{N} \nu_j^{(i)} R_j \qquad q_i = \sum_{j=1}^{N} \nu_j^{(i)} Q_j \tag{11}$$

where $\nu_j^{(i)}$ is the number of groups of type j present in molecule i.

The dependency on T_{dp} of the activity coefficients is given by the *residual* part, computed according to UNIFAC by

$$\ln \gamma_i^R = \sum_{k=1}^{M} \nu_k^{(i)}[\ln \Gamma_k - \ln \Gamma_k^{(i)}] \tag{12}$$

where M is the number of groups present in the liquid mixture. In our case, the only groups present in the n-alkane mixture are CH_3 and CH_2, and thus $M = 2$.

The functions Γ_k have been calculated according to

$$\ln \Gamma_k = Q_k\left(1 - \ln B_k - \sum_{j=1}^{M} \frac{\Theta_j \Psi_{kj}}{B_j}\right) \tag{13}$$

In the former equation, the interaction parameter Ψ_{kj} is given in terms of the binary interaction energies (A_{kj}, in K) between groups k and j and the dew-point temperature by

$$\Psi_{kj} = \exp\left(-\frac{A_{kj}}{T_{dp}}\right) \tag{14}$$

On the other hand, the parameter Θ_j represents the molar area of group j in the mixture, and is given by

$$\Theta_j = \frac{X_j Q_j}{\sum_{k=1}^{M} X_k Q_k} \qquad \text{with} \qquad X_j = \frac{\sum_{i=1}^{N} \nu_j^{(i)} x_i}{\sum_{k=1}^{M}\sum_{i=1}^{N} \nu_k^{(i)} x_i} \tag{15}$$

and finally B_j is given by

$$B_j = \sum_{k=1}^{M} \Theta_k \Psi_{kj} \tag{16}$$

Equation 13 also gives the reference functions $\Gamma_k^{(i)}$, which correspond to the value of Γ_k of each group k in a mixture that contains only the component i.

Continuum Approximation. To calculate the activity coefficients in the continuum approximation, the index that corresponds to a chemical species in the mixture is considered as a continuous variable. Choosing the carbon number parameter n as the variable that describes the composition [equivalent to the molecular weight (MW)], we have the substitution $F_i \rightarrow F(n)$, for a generic function F. Accordingly, the corresponding sums with respect to those indexes are approximated by integrals according to

$$\sum_{i=1}^{N} F_i \rightarrow \frac{N}{N-1}\int_{n_{\min}}^{n_{\max}} F(n) dn \tag{17}$$

On the other hand, the index that corresponds to the groups present in the mixture remains as a discrete variable because the number of different groups is small.

Thus, the activity coefficients in the continuum approximation are calculated by inserting the substitution rule Eq. 17 in Eqs. 8–16, for all the sums over the chemical species present in the mixture.

Basic data for the n-alkanes

To carry out the calculations in the CMT approximation, the thermophysical properties involved have to be specified as continuous functions of the carbon number (n), which have to be "extrapolated" from the discrete data corresponding to the chemical species. A convenient way to perform such extrapo-

Table 1. Fuel Parameters Considered for the Exterior Gas Composition in Eq. 18

Fuel Blend	α	β (g/mol)	γ (g/mol)	$n_{\min}$	$n_{\max}$	N	y_∞^F
JP4	16.9	6.7	0	5	16	12	0.05
Gasoline	5.7	15	0	5	18	14	0.05
Diesel	18.5	10	0	5	25	21	0.05

lation[7] is to correlate the discrete data as a function of n, using simple formulas (such as power laws) with physical meaning.

Bulk Gas Composition. The exterior gas composition has been approximated to a continuous mixture of n-alkanes, specified here (in mole fraction) by the Gamma distribution function, renormalized to take into account that the domain of variation of M_n is limited to a finite interval (see Table 1). Thus, the PDF for the mole fractions in the bulk gas is given by

$$y_\infty(n) \propto \left(\frac{M_n-\gamma}{\beta}\right)^{\alpha-1}\exp\left(-\frac{M_n-\gamma}{\beta}\right) \tag{18}$$

where M_n is the molecular weight of C_nH_{2n+2} and the proportionality factor missing is determined by the normalization condition

$$y_\infty^F = \frac{N}{N-1}\int_{n_{\min}}^{n_{\max}} y_\infty(n)dn \tag{19}$$

For our numerical illustrations the total fuel mass fraction in the bulk gas has been taken as $y_\infty^F = 0.05$. The values of the parameters α, β, and γ, corresponding to the fuels JP4, gasoline, and diesel, have been taken from Hallett[14] and are given in Table 1.

Saturation Pressures. The saturated vapor pressure has been determined as a function of the carbon number using the Antoine equation

$$p^{sat}(n) = \exp\left[A(n)-\frac{B(n)}{T-C(n)}\right] \quad \text{(MPa)} \tag{20}$$

where the functions $A(n)$, $B(n)$, and $C(n)$ have been correlated[7] by means of a power law, from data[15] for $5 \le n \le 16$, as follows

$$A(n) = 6.318n^{0.05091}$$

$$B(n) = 1178n^{0.4652} \quad \text{(K)}$$

$$C(n) = 9.467n^{0.9143} \quad \text{(K)} \tag{21}$$

The above-mentioned value of $n_{\max}$ implies that some of our calculated saturation pressures (especially for diesel fuel) are based on a modest extrapolation of data for smaller carbon numbers. This will be accepted for our present purposes because our main goal here is to analyze/illustrate the use of several alternative CMT-based methods when using the same basic data.

The numerical results shown here (including the numerical integrations and these correlations) were derived with *Mathematica* using 16 figures. Although the precision of the experimental data for the present correlations is, in most cases, $<10^{-4}$, the numerical results presented here have been rounded to four significant figures.

Soret Factors Used. The average thermal diffusion coefficient of each component is given, in terms of the corresponding Schmidt number (Sc), by[10]

$$\alpha_T(n) = \frac{3}{4}\left(1+\frac{\pi}{8}\right)^{-1}\left(\mathrm{Sc}_n-\frac{3}{4}\right)\left(1-\frac{T_{Cn}}{T_{\mathrm{BL}}}\right) \tag{22}$$

where the crossover temperature is given as a function of carbon number by

$$T_{Cn} = 186\left(\frac{M_n}{M_{n=12}}\right)^{0.3669} \tag{23}$$

In the former expression, the Schmidt number of each component has been computed as

$$\mathrm{Sc}_n = \mathrm{Sc}_{n=12}\left(\frac{M_n}{M_{n=12}}\right)^{0.654} \tag{24}$$

where the Schmidt number of n-dodecane is given, as a function of the average BL temperature in the vicinity of the condenser surface, by

$$\mathrm{Sc}_{n=12} = 2.627+\left(\frac{T_{\mathrm{BL}}}{207.721}\right)^{-1.54774} \tag{25}$$

Activity Coefficient Data. The data needed to compute the activity coefficients[11] are given by the following system of equations

$$R_j = \{0.9011,\ 0.6744\} \qquad Q_j = \{0.848,\ 0.540\}$$

$$A_{jk} = \begin{pmatrix} 0 & 86.02 \\ -35.36 & 0 \end{pmatrix}\mathrm{K} \qquad \nu_j^{(n)} = \{2,\ n-2\} \tag{26}$$

where the first entry in the former arrays corresponds to the group CH_3 and the second to the group CH_2.

LFL Data; Le Chatelier Mixing Rule and T-Dependency. From an explosion/flammability perspective an important consideration for hydrocarbon vapor is its so-called lean (or lower) flammability limit (LFL_{mix}), expressed here as its mole fraction in air at the p, T conditions of interest. Concentrations lower than this are presumed to be safe to work with even in the presence of potential ignition sources.

LFL estimates for fuel blends are often successfully made

using the so-called Le Chatelier mixing rule, according to which

$$\mathrm{LFL}_{mix} = y_w^F \left(\sum_{i=1}^{N} \frac{y_w^i}{\mathrm{LFL}_i} \right)^{-1} \tag{27}$$

where y_w^F is the total fuel mole fraction at the condenser surface and y_w^i are the corresponding mole fractions of the various discrete fuel components at the surface. The CMT limit version of this relation is clearly

$$\mathrm{LFL}_{mix} = y_w^F \left[\frac{N}{N-1} \int_{n_{\min}}^{n_{\max}} \frac{y_w(n)}{\mathrm{LFL}(n)}\, dn \right]^{-1} \tag{28}$$

where, in the present case, $y(n)$ represents the L-S distorted, renormalized Gamma distribution function given by Eq. 6.

The lower or lean flammability limit of each of the *n*-alkane fuel vapors is well known at 1 bar, 300 K. Indeed, Yaws' compendium[16] provides the following systematic dependency on carbon number n

$$\mathrm{LFL}(n, 300\ \mathrm{K}) \simeq \frac{0.55}{4.76n + 1.19(2n+2) + 1} \tag{29}$$

In the present case, to assess the local flammability of the *n*-alkane vapor mixture formed at T_{dp}, we need to be able to predict LFL(n, T) for temperatures > 300 K. Fortunately, this is readily estimated based on the observation that the adiabatic flame temperature for lower-limit mixtures is approximately constant. This provides the rational extrapolation formula[2]

$$\mathrm{LFL}(n, T) \simeq \mathrm{LFL}(n, 300\ \mathrm{K}) - \frac{\langle C_p \rangle (T - 300\ \mathrm{K})}{Q_c(n)} \tag{30}$$

Here $Q_c(n)$ is the molar (and "lower") heat of combustion of the alkane vapor, and $\langle C_p \rangle$ is an appropriate mean molar heat capacity [estimated here to be close to 32.5 J gmol^{-1} K^{-1}, based on *air* properties (thus independent of n)]. Of course, for self-consistency (see footnote 2), T must be low enough that all of the relevant LFL(n, T) values remain positive. Combining the above relationships it clearly becomes possible to assess the flammability of the *n*-alkane vapor mixture established near the surface at the converged temperature T_{dp}. Explicitly, we compare $\mathrm{LFL}_{mix}(T_{dp})$ as calculated above to the value of y_w^F, given by Eq. 7, where y_∞^Fwill be specified. Such straightforward results will also be included in our results section.

In the CMT calculations, the heat of combustion is given as a function of n by means of the correlation,[7] based on the data (for $n \leq 20$) from[18]

$$Q_c(n) \simeq M_n 43.84 \left(1 + \frac{0.1729}{n} \right) \qquad (\mathrm{MJ\ mol^{-1}}) \tag{31}$$

[2] This relation corrects the unreasonable version quoted (without its basis) in a recent book by Seider et al.[17]

Inferences Based on Pure Liquid Viscosities (Condensate Fluidity). We seek to estimate the effect of our model assumptions (such as incorporating Ludwig–Soret species separation in the vapor phase) on the viscosity of the incipient liquid condensate. For example, this information would be of interest for predicting condensate runoff resulting from gravity and/or gas shear (see, for example, Rosner et al.[19]), or for predicting solute diffusion through such films. Although there seem to be no generally useful "mixing rules" for liquid viscosity (with respect to the situation for gas mixture viscosity[9]) the following approximate method will be adequate for our present purposes. If the condensate viscosity were considered to be a function only of its temperature and mean carbon number, then any phenomenon that causes a fractional change in T_{dp} and/or mean carbon number will cause a corresponding fractional change in viscosity that can be estimated using pure component viscosity data. Thus, when these fractional changes are dT_{dp}/T_{dp} and $d\bar{n}/\bar{n}$, respectively, we report the corresponding fractional change in condensate viscosity as

$$\frac{d\mu_L}{\mu_L} = \frac{\partial \ln \mu_L}{\partial \ln T} \frac{dT_{dp}}{T_{dp}} + \frac{\partial \ln \mu_L}{\partial \ln n} \frac{d\bar{n}}{\bar{n}} \tag{32}$$

where the indicated sensitivity coefficients $\partial \ln \mu_L / \partial \ln T$ and $\partial \ln \mu_L / \partial \ln n$ are calculated from the component viscosity correlations reported in Yaws,[16] evaluated[3] at T_{dp} and $\bar{n}$. It is interesting to note that in the present class of applications these individual contributions act in opposite directions—that is, although Ludwig–Soret vapor separation facilitates condensation (raises T_{dp}, thus lowering the viscosity), the increased mean molecular weight (or carbon number) in the incipient condensate acts to increase the viscosity. In all of the present cases, the first effect was found to dominate, so that inclusion of L-S enrichment in the vicinity of the cooled surface leads to incipient condensates of systematically lower viscosity ($\sim$12% in typical cases).

Continuous mixture approach to the prediction of T_{dp} and associated condensate composition

There are several possible ways of dealing with Eq. 3, reexpressing the VLE condition in the CMT approximation. A method that is especially interesting when only the lowest-order moments of the condensate composition PDF [$x(n)$] are relevant, is the so-called method of moments (or MOM). In the MOM, Eq. 3 is replaced by a finite set of "moment" equations, obtained by multiplying both sides by n^k, where k is frequently a positive integer, and then integrating over the domain [$n_{\min}$, $n_{\max}$], which leads to the following set of integral equations

$$\int_{n_{\min}}^{n_{\max}} n^k \gamma(n, T_{dp})\, x(n) dn = \int_{n_{\min}}^{n_{\max}} \frac{n^k y_w(n) p}{p^{sat}(n, T_{dp})}\, dn \qquad k = 0, 1, 2, \cdots \tag{33}$$

[3] For the cases reported in the present paper (JP4, gasoline, and diesel fuels, Table 1), the mean carbon number in the condensate was never far from 13, 15, and 20, respectively. For this reason, the sensitivity coefficients used for our present condensate viscosity estimates were simply taken to be those for tridecane (−3.98, 1.89), pentadecane (−4.12, 2.01), and eicosane (−3.82, 1.60), respectively.

where the righthand side (RHS) is a specified function of the dew-point temperature.

Clearly, if one specified the functional form of the condensate PDF (say a two-parameter Gamma distribution, with or without lower- and upper cutoffs), then three such moment equations would be sufficient to determine T_{dp} together with the two parameters appearing in this Gamma distribution representation. Although this method is attractive because of its simplicity (especially when $n_{\max} = \infty$), we seek/explore here more general methods that are explicitly *free of a restrictive presumption about the shape of the PDF*—indeed, because of the nature of the functions $p^{sat}(n, T)$, $\alpha_T(n)$, and the activity coefficients $\gamma(n, T)$, the function $x(n)$ is expected to systematically depart from the specified mainstream PDF. Because condensate properties are often quite sensitive to both T_{dp} and the PDF $x(n)$, such methods will be required for solving more complex multiphase transport problems. A MOM that does not restrict the mathematical form of the condensate PDF is the quadrature method of moments (QMOM),[20] which is illustrated in more detail below.

A variant of MOM that does not involve the calculation of moments and does not restrict the mathematical form of the condensate PDF is the use of a "spectral representation" of the condensate PDF.[7,21-25] In this case, the condensate PDF is expanded in terms of a complete basis of the functional (Hilbert) space of square integrable functions over the domain $[n_{\min}, n_{\max}]$ (that is, $L^2[n_{\min}, n_{\max}]$), and the coefficients of the expansion are determined from the corresponding spectral expansion of Eq. 3, which constitutes the basis of the spectral orthogonal collocation (SOC) method (see below).

Moment Formulation for the Case of a Presumed PDF in the Condensate. Let us assume that the composition of the condensate is given by a presumed mathematical form PDF (f^L), depending on, say, two parameters α and β. Then recalling Eq. 4 we have

$$x(n) = \left(1 - \frac{1}{N}\right) f^L(n;\, \alpha,\, \beta) \tag{34}$$

where the PDF $f^L(n;\, \alpha,\, \beta)$ is normalized in the interval $[n_{\min} n_{\max}]$. Inserting the former definition in Eq. 33 with $k = 0$, 1, and 2 we find the closed system for the three unknowns T_{dp}, α, and β

$$\int_{n_{\min}}^{n_{\max}} f^L(n; \alpha, \beta)\gamma(n, T_{dp})dn = \int_{n_{\min}}^{n_{\max}} \frac{f^G(n)p}{p^{sat}(n, T_{dp})}\, dn$$

$$\int_{n_{\min}}^{n_{\max}} nf^L(n; \alpha, \beta)\gamma(n, T_{dp})dn = \int_{n_{\min}}^{n_{\max}} \frac{nf^G(n)p}{p^{sat}(n, T_{dp})}\, dn$$

$$\int_{n_{\min}}^{n_{\max}} n^2 f^L(n; \alpha, \beta)\gamma(n, T_{dp})dn = \int_{n_{\min}}^{n_{\max}} \frac{n^2 f^G(n)p}{p^{sat}(n, T_{dp})}\, dn \tag{35}$$

where the gas-phase PDF $f^G(n)$ is defined by

$$y_w(n) = \left(1 - \frac{1}{N}\right) f^G(n) \tag{36}$$

and is a function of the dew-point temperature determined explicitly by Eq. 6. In a general case, the integrals appearing in the former system of equations cannot be computed analytically, which prevents the analytical application of the MOM. However, this difficulty can be overcome by evaluating these integrals using any suitable numerical scheme, such as Gaussian quadrature formulae (GQF), for instance.

Moment Formulation for the General Case with N_Q Gaussian Quadrature Points: QMOM. The QMOM is a *moment-based* method in which the liquid composition PDF is not restricted to a particular mathematical family; instead a general PDF [$f^L(n)$], normalized in the interval of interest, is considered. In this case, the system is closed by evaluating the integrals involving $f^L(n)$ by means of the GQF, defined in the interval $[n_{\min}, n_{\max}]$, which has the unknown PDF [$f^L(n)$] as the weight function, that is (in the case of N_Q Gaussian quadrature points),

$$\int_{n_{\min}}^{n_{\max}} f^L(n)\, g(n)dn \simeq \sum_{j=1}^{N_Q} W_j g(n_j) \tag{37}$$

where $g(n)$ is any generic function of n. The N_Q abscissae $\{n_j\}_{j=1}^{N_Q}$ and weights $\{W_j\}_{j=1}^{N_Q}$ are determined in terms of the first $2N_Q$ moments of the (unknown) PDF f^L

$$\langle n^k \rangle = \int_{n_{\min}}^{n_{\max}} n^k f^L(n)dn \qquad k = 0, \ldots, 2N_Q - 1 \tag{38}$$

by the system of equations

$$\sum_{j=1}^{N_Q} W_j n_j^k = \int_{n_{\min}}^{n_{\max}} \frac{n^k f^G(n)p}{\gamma(n, T_{dp})p^{sat}(n, T_{dp})}\, dn \qquad k = 0, \ldots, 2N_Q - 1 \tag{39}$$

which can be efficiently solved by means of the product-difference algorithm.[20] In this case, the normalization condition for the liquid composition PDF is given by

$$\sum_{j=1}^{N_Q} W_j = 1 \tag{40}$$

and closes the former system for the abscissae, weights, and dew-point temperature.

In the former system, the integrand appearing on the RHS is a known function of the dew-point temperature, and the integrals can be carried out by means of any suitable numerical scheme, such as a GQF.

Spectral Orthogonal Collocation (SOC) Method. In this method the PDFs of the problem are approximated by means of a truncated spectral expansion with $\hat{N}$ components

$$x(n) \simeq \sum_{i=1}^{\hat{N}} \hat{x}_i \varphi_i(n)$$

$$y_w(n) \simeq \sum_{i=1}^{\hat{N}} \hat{y}_i \varphi_i(n) \tag{41}$$

based in *any* complete basis set ($\{\varphi_i\}_{i=1}^{\infty}$) of the functional (*Hilbert*) space of square integrable functions over the domain of interest ($L^2[n_{\min}, n_{\max}]$). In general, it is always possible to choose a basis $\{\varphi_i\}_{i=1}^{\infty}$ that is *orthonormal* with respect to the scalar product, defined by a certain "weight" function $\Omega(n) > 0$

$$(\varphi_i, \varphi_j) \equiv \int_{n_{\min}}^{n_{\max}} \Omega(n)\varphi_i(n)\varphi_j(n)dn = \delta_{ij} \tag{42}$$

In that case, the coefficients of the expansion are given by the corresponding spectral projections

$$\hat{x}_i = (\varphi_i, x) = \int_{n_{\min}}^{n_{\max}} \Omega(n)\varphi_i(n)x(n)dn \tag{43}$$

Thus, the coefficients of the gas composition PDF $\hat{y}_i$ are known functions of the dew-point temperature, and the coefficients of the liquid composition $\hat{x}_i$ are the new unknowns of the problem.

Given that, by definition, the PDF belongs to $L^2[n_{\min}, n_{\max}]$, the former approximation is exact in the limit $\hat{N} \to \infty$ for any basis; however, the rate of convergence depends on the choice of basis and on the smoothness of the PDF and its derivatives. Without additional information about the shape of the PDF, a good choice of basis is given by the Chebyshev polynomials [which are orthogonal in $[-1, 1]$ with respect to $\Omega(n) = (1 - n^2)^{-1/2}$] scaled to the interval of interest. With this choice, and in the case of smooth PDFs (as those of interest here), the former truncated expansion is reasonably accurate, in terms of local values of the PDF, with as few as $\hat{N} = 3$ spectral components and becomes very accurate for $\hat{N}$ values between 6 and 10.

In the SOC method the coefficients of the expansion of the unknown PDF ($\hat{x}_i$) are determined by minimizing the error (or "residual") arising from the truncation in the former expansions [$\xi(n)$] in a global way over the domain of interest. This is done by approximating the *norm* of the residual by the GQF associated with the chosen basis

$$\|\xi\|^2 \equiv \int_{n_{\min}}^{n_{\max}} \Omega(n)[\xi(n)]^2 dn \simeq \sum_{i=1}^{\hat{N}} \Omega_i[\xi(n_i)]^2 \tag{44}$$

and imposing

$$\xi(n_i) = 0 \qquad i = 1, \ldots, \hat{N} \tag{45}$$

which leads to $\|\xi\|^2 \approx 0$ according to Eq. 44. In the former GQF, the abscissae (n_i) are given by the $\hat{N}$ roots of the first basis element not included in the expansion ($\varphi_{\hat{N}+1}$), and the weights (Ω_i) are easily calculated taking into account that the GQF is exact for polynomials of degree $\leq 2\hat{N} - 1$.

Thus, in SOC the system of equations that determines the coefficients of the truncated expansion of $x(n)$ is found by inserting the spectral expansion Eq. 41 in Eq. 3 and evaluating the resulting equation at the $\hat{N}$ fixed abscissae defined by $\varphi_{\hat{N}+1}(n_i) = 0$:

$$\gamma(n_i, T_{dp})\, x(n_i)\, p^{sat}(n_i, T_{dp}) = y_w(n_i)\, p \qquad i = 1, \ldots, \hat{N} \tag{46}$$

where substitution of Eq. 41 in Eq. 4 gives the additional equation that closes the system for $\hat{x}_i$ and T_{dp}. Thus, the original mixture of N physical components is, in effect, approximated by a mixture of $\hat{N} \ll N$ pseudo-components, chosen according to a mathematically rational and well-defined (convergent) scheme.

SOC is simpler to implement that QMOM because it simply involves the *evaluation* of the original governing equations at a certain fixed set of abscissae or pseudo-components, and does not involve the calculation of *moments*. Moreover, SOC directly gives an approximation of the whole PDF (Eq. 41), which can be used to compute any desired moment. Further details about the *efficient* implementation of SOC in terms of *cardinal functions* can be found in Arias-Zugasti and Rosner[7] and Boyd.[25] The results obtained with SOC presented here have been computed by means of the former scheme (implemented efficiently in terms of *cardinal functions*), using $\hat{N}$ Chebyshev nodes scaled to the domain of interest.

Numerical methods: first approximations, iterative procedures, and convergence

In all cases (with/without L-S transport), the calculation is started considering the liquid mixture as ideal. This leads to a first approximation of the dew-point temperature and liquid composition, which is used to calculate the activity coefficients. The calculation is then repeated based on these activity coefficients, which leads to a new estimation of T_{dp} and liquid composition. The process is iterated until the sum of the differences (in absolute value) in T_{dp} and all the parameters that specify the liquid composition, from one iteration to the next, is $<10^{-6}$. In this respect, the number of iterations needed to attain convergence was about five in all the cases.

Results for Predicted Dew Points and Corresponding Condensate Composition

The former three methods have been applied to solve the canonical isobaric dew-point problem for the cases of JP4, gasoline, and diesel fuels in a N_2 gas stream (see Table 1 for exterior gas composition). To make comparisons between these CMT-based methods and the *exact* solution, corresponding to the *discrete* mixture, the problem has also been solved without making use of the *continuous* approximation. The results for dew-point temperature (T_{dp}) and gas/liquid mean carbon number composition ($\bar{n}^G/\bar{n}^L$) and spread ($\Delta n^G/\Delta n^L$), are summarized in Table 2. The results for mixture lower flammability limit and relative variation in liquid viscosity between the calculations, with and without accounting for L-S separation, can also be found in Table 2.

In all the cases considered, the nonideality of the liquid condensate is very moderate, and the variations induced by

Table 2. Discrete Mixture (Exact) Results

	JP4		Gasoline		Diesel	
	Ideal	Nonideal	Ideal	Nonideal	Ideal	Nonideal
T_{dp} (K)						
L-S no	358.0	358.2	372.3	372.6	470.4	470.7
L-S yes	368.7	369.0	382.6	382.9	482.5	482.8
n^G						
L-S no	8.009	8.009	7.163	7.163	13.04	13.04
L-S yes	8.161	8.161	7.355	7.354	13.24	13.24
n^L						
L-S no	12.60	12.57	15.31	15.23	20.44	20.39
L-S yes	12.50	12.47	15.17	15.08	20.25	20.20
Δn^G						
L-S no	1.887	1.887	2.111	2.111	3.050	3.050
L-S yes	1.922	1.922	2.214	2.213	3.079	3.079
Δn^L						
L-S no	2.391	2.425	2.770	2.862	3.453	3.506
L-S yes	2.388	2.421	2.813	2.902	3.476	3.528
LFL						
L-S no	0.00871	0.00871	0.00958	0.00957	0.00503	0.00503
L-S yes	0.00849	0.00849	0.00927	0.00927	0.00490	0.00490
$\Delta\mu^L/\mu^L$	−0.131	−0.131	−0.130	−0.130	−0.111	−0.111

Note: The columns labeled with ideal/nonideal correspond to the approximation of ideal and nonideal liquid mixtures, respectively. The rows labeled with L-S no/L-S yes have been calculated by neglecting/including L-S transport, respectively.

Soret separation predominate strongly over those introduced by nonideality. The shifts introduced by Soret transport on dew-point temperatures (~10 K in all cases) are quite remarkable. As a consequence of this increase in T_{dp}, a reduction of nearly 3% in LFL is observed, and a reduction in condensate viscosity between 11 and 13% is found.

CMT results: presumed mathematical form PDF

As mentioned earlier, once a shape for the liquid composition PDF is assumed and a numerical scheme is introduced to approximate the integrals, the problem, for a two-parameter distribution, reduces to a system of three nonlinear equations in the three unknowns: T_{dp}, α, and β. A 10-point Gaussian quadrature and a Newton iterative solver were used to approximate the integrals and solve the resulting nonlinear system. Convergence was achieved only when the shape of the PDF was well chosen and sufficiently accurate initial guesses were used for T_{dp} and PDF parameters. Liquid composition at incipient condensation is often quite different from that of a gaseous one even in the case of negligible nonideality and thermal diffusion effects; the first drop of liquid that forms is much richer in heavier components because of vapor pressure disparities. In this case, where the gas composition was modeled using a two-parameter Gamma distribution, the same PDF could not by any means succeed in describing the liquid composition, but a strongly right skewed PDF had to be used; a Beta distribution that allows for great flexibility in modeling was chosen. Initial guesses for T_{dp} have been taken equal to those of mixtures of inert carrier gas and one component fuel ($y^F_\infty = 0.05$) of carbon number equal to the average one of the fuel blend; initial guesses for the PDF parameters have been generated by fitting a Beta distribution through the one obtained for the liquid composition in the discrete case.

The results show that the accuracy of the method is not affected by the inclusion of thermal diffusion and liquid nonideality, whereas it can vary quite appreciably depending on mainstream gas composition. Good agreement with the exact solution was obtained for JP4 and diesel, whereas the results obtained for gasoline are less accurate.

Dew-point temperatures were estimated with a relative error of <1% in the best two cases (JP4 and diesel) and of about 5% in the worst one (gasoline). In all cases the results for gas and liquid composition are less accurate than those for T_{dp}, with relative errors from 1 to 8% for the mean carbon number and from 3 to 11% for the spread. The presumed PDF results for the condensate compositions can be seen in Figure 1; a comparison with those in Figure 5 (see below) obtained by means of the more accurate SOC method suggests that in the case of gasoline the presumed Beta distribution shape does not work quite as well as in the other two cases in describing the liquid composition distribution.

It can be concluded that ease of implementation and lower computational cost are certainly attractive features of the presumed PDF method, although accuracy and convergence are not guaranteed, especially when reasonable initial estimates cannot be generated based on experience.

CMT results: general form PDF (QMOM and SOC)

The results found by means of the two general mathematical form PDF methods considered here (QMOM and SOC) show very good agreement with the *exact* results (Table 2) in all cases.

One of the most important features of the general form PDF methods, is their *convergence* as the number of abscissae (N_Q and$\hat{N}$) is increased. In fact, the possibility of improving the approximation until convergence is reached is the main difference between these methods and the presumed mathematical form PDF method. To illustrate the improvement of the results as the number of abscissae increases, the results for dew-point temperature and gas/liquid mean composition and spread are shown, as a function of the number of abscissae, in Figures 2, 3, and 4, respectively.

The first important consequence that can be derived from these results is that, in all the cases considered here (that is, for all the

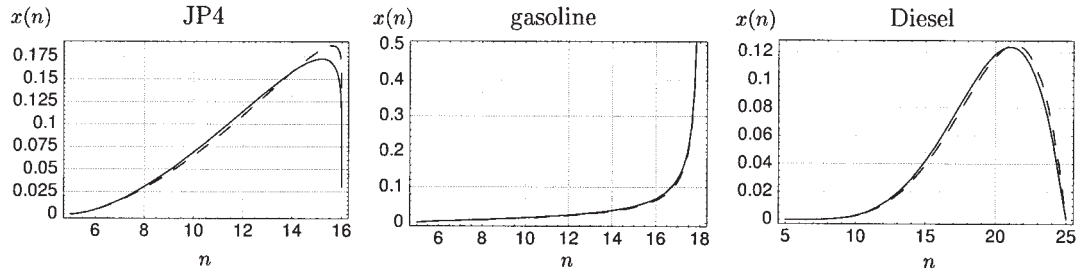

Figure 1. Condensate composition vs. carbon number *n*, computed by means of the presumed mathematical form method for the three fuels considered.

The dashed lines correspond to the calculation neglecting L-S transport, and the solid lines to the calculation including L-S transport. The present results correspond to approximation of an ideal liquid mixture; the results corresponding to the nonideal liquid mixture are practically identical.

fuels, with/without L-S separation, with/without liquid nonideality), the *accuracy* and *rate of convergence* of both methods are remarkably similar and high. In both cases the results become very accurate in the range of three to four abscissae, and convergence is reached for six to seven abscissae.

The dew-point temperatures are especially accurate. The results for T_{dp} corresponding to both QMOM and SOC, with only one abscissa, have a relative error of $<5\%$ in all cases, which falls to 1% in the range of two to three abscissae, and finally becomes of the order of 0.1% when four to five abscissae are considered.

The QMOM and SOC results for gas and liquid composition are not as accurate as those for T_{dp}, but are still quite accurate. The results for mean carbon number show a relative error of 10% in the range of two to three abscissae, decreasing to 1% when four or more abscissae are considered. The results for average carbon number spread show a relative error of 30% in the range of two to three abscissae, decreasing to 3% when four or more abscissae are considered.

In the cases considered here both QMOM and SOC lead to results with very similar accuracy and rate of convergence. However, the computational load of QMOM is much greater than that of SOC, resulting in computation times several times larger. SOC is a very fast and efficient spectral method, although application of SOC is limited to those cases in which all the PDFs under consideration (and their derivatives) are smooth functions. Otherwise, the well-known Gibbs phenomenon is found, and SOC cannot be used. Another limitation of SOC is that the *region of interest* (the interval where the PDF is appreciably greater than zero) has to be known beforehand. This is because in SOC (once the weight function Ω is chosen) the abscissae are determined by the *working* interval and *fixed*. As a consequence, if the region of interest is not known, the number of abscissae needed to represent a PDF over an interval larger than the region of interest is usually too large for SOC to be applicable. Within these limitations SOC is a very efficient method, which provides not only moments of the PDF, but the PDF itself as an analytical function of the independent variable (see Eq. 41 and Figure 5). This analytical function can be used to calculate any function of the PDF, including *global* functions (such as moments) and *local* functions (such

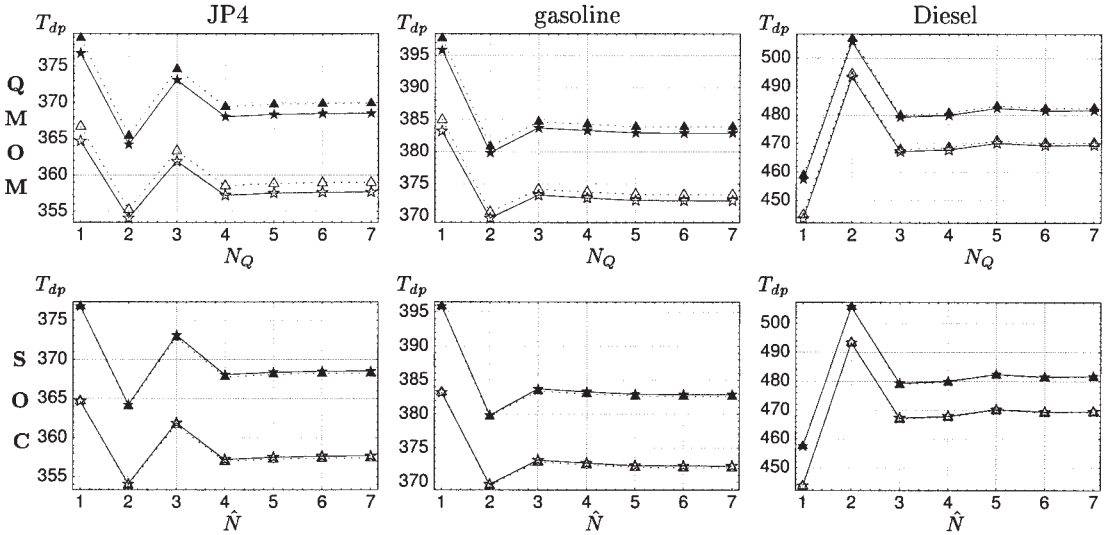

Figure 2. Dew-point temperatures (K) vs. number of "pseudo-components" used in the calculation.

Each column corresponds to a fuel blend [JP4 (left), gasoline (center), diesel (right)], and each row to a method [QMOM (top), SOC (bottom)]. The triangles joined with dotted lines correspond to the approximation of an ideal liquid mixture; the stars joined with solid lines, to the nonideal liquid mixture. The filled triangles/stars correspond to the calculation including L-S transport, and the hollow symbols to the calculation without L-S transport.

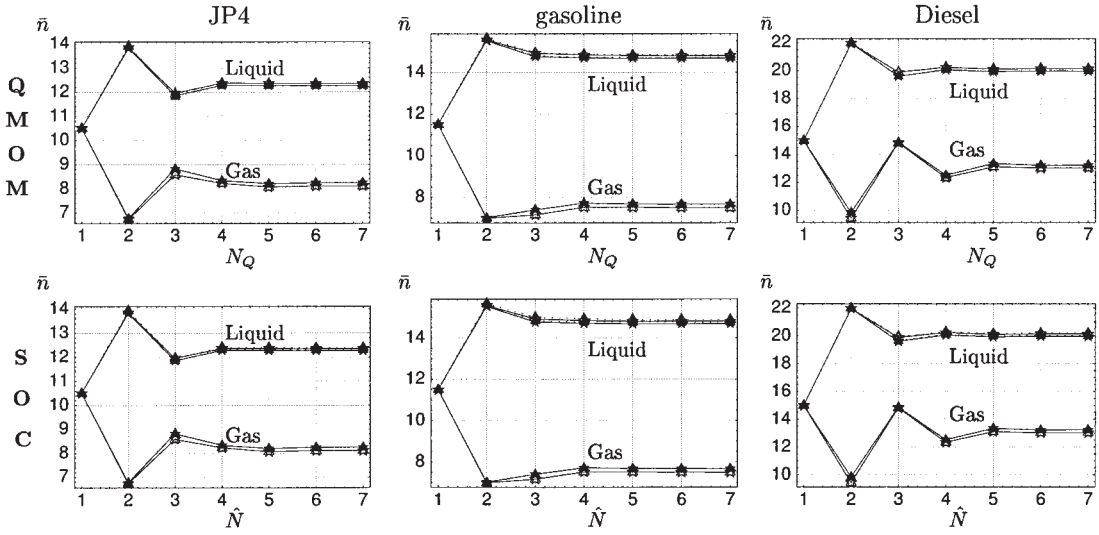

Figure 3. Average carbon number vs. number of "pseudo-components" used in the calculation.

Each column corresponds to a fuel blend and each row to a method. The triangles/dotted lines correspond to the ideal liquid mixture and the stars/solid lines to the nonideal liquid mixture. The filled/hollow symbols correspond to the calculation with/without L-S transport.

as the values of the PDF at the *real* components, and/or the derivatives of the PDF).

QMOM, on the other hand, is more computationally demanding than SOC, but has the important advantages that it is not limited to smooth PDFs and it does not require any a priori knowledge about the region of interest, because in QMOM the abscissae are determined by the PDF itself. As a consequence, the domain of application of QMOM is much broader than that of the present version of SOC.

All the cases studied here have intervals of interest known beforehand and fixed, and all the PDFs involved are very smooth, making SOC more advantageous over QMOM, in terms of computation times and ease of implementation. On the other hand, our results show that QMOM is as accurate as SOC, and has the same rate of convergence in terms of number of abscissae.

In a general case, depending on the smoothness of the PDFs involved and on the available knowledge about the region of interest, either SOC or QMOM will be more convenient. The development of a general method that combines the good features of both SOC and QMOM is one of our present lines of research.

Validity of assumption A4 (solubility of N_2 in condensate)

The solubility of N_2 in this type of multicomponent condensate ($\gamma \leq 1$) is bounded by

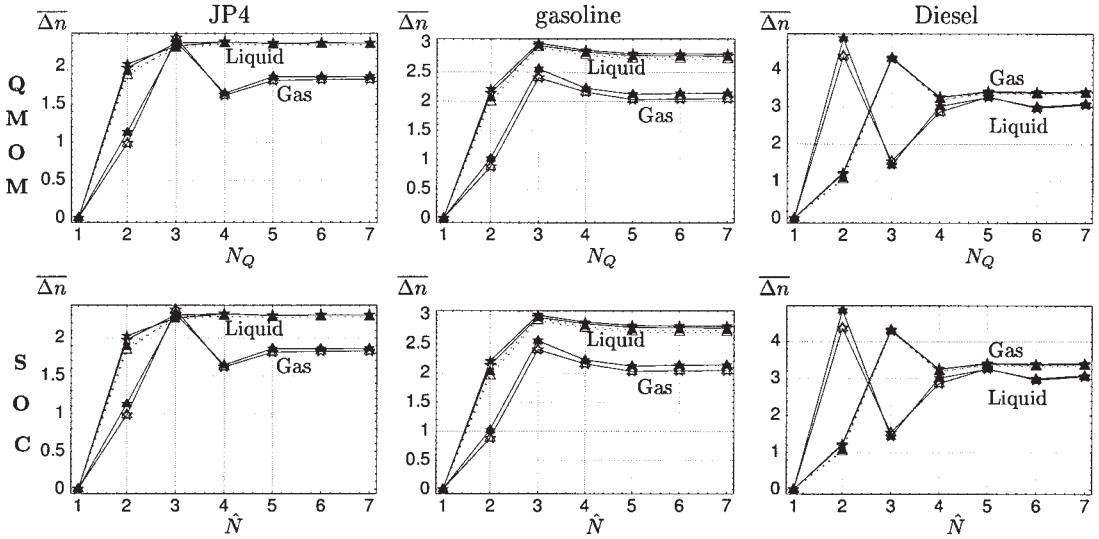

Figure 4. Average carbon number spread vs. number of "pseudo-components" used in the calculation.

Each column corresponds to a fuel blend and each row to a method. The triangles/dotted lines correspond to the ideal liquid mixture and the stars/solid lines to the nonideal liquid mixture. The filled/hollow symbols correspond to the calculation with/without L-S transport.

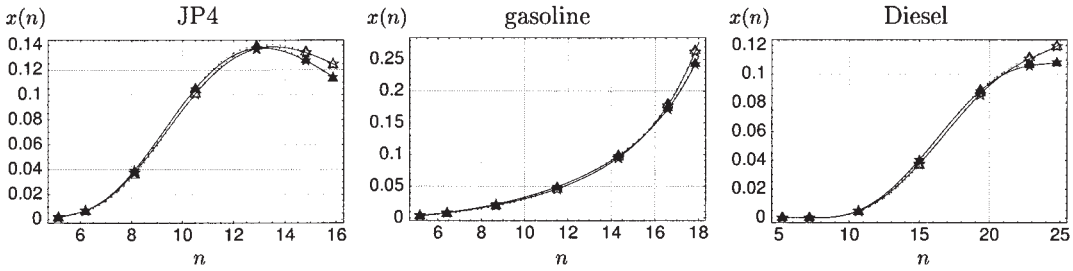

Figure 5. Condensate composition vs. carbon number *n*, computed by means of the spectral orthogonal collocation method (Eq. 41) with $\hat{N}$ "pseudo-components."

The triangles/dotted lines correspond to the ideal liquid mixture and the stars/solid lines to the nonideal liquid mixture. The filled/hollow symbols correspond to the calculation with/without L-S transport.

$$\frac{x_{N_2}}{y_{N_2,w}} \leq p \exp\left[-\frac{N}{N-1} \int_{n_{\min}}^{n_{\max}} \ln H(n) x(n) dn \right] \qquad (47)$$

where $H(n)$ is the relevant pure solvent Henry constant. According to this result, the solubility of N_2 in the condensate, at the pressures and dew-point temperatures of interest, is estimated to be <0.002 in all cases considered, confirming our assumption A4.

Validity of the "continuous representation" of the n-alkane mixture

The continuous approximation, performed in all the CMT-based methods, introduces an error that is expected to decrease as the number of components increases. As a consequence, both general-form PDF methods (QMOM and SOC) converge to a solution that is *systematically different* from the exact (discrete N component mixture) solution. An important question is then the *minimal* number of components needed for the continuous approximation to be acceptable.

In this respect, the QMOM and SOC results presented here show, in all the cases considered, only marginal (negligible) variations in rate of convergence and final (converged) relative errors as the number of components, in the real (discrete) mixture, increases from $N = 12$ (JP4) to $N = 21$ (diesel). As a consequence, taking into account that our CMT results are quite accurate, we may conclude that a number of discrete components of order 10 is already large enough for the continuous representation to be a good and useful approximation.

Broader Conclusions and Recommendations

Summary of basic CMT methods and principal conclusions

Three rather efficient continuous mixture-based computational methods have been proposed/illustrated for the present canonical dew-point problem. Two of the methods are "moment based," and all exploit Gaussian quadratures. The first method presumed the functional form of the concentration distribution function in the incipient condensate (such as a two-parameter "Beta" PDF), and simply calculates the parameters entering this PDF (such as MMW and MW spread), in addition to the associated value of T_{dp}. A second, more general method, now called a "quadrature method-of-moments" (QMOM), yielded both the dew-point temperature and a systematic multi-delta-function approximation to the actual liquid-phase PDF. The third method illustrated (see, also Arias-Zugasti and Rosner[7])—the "spectral orthogonal collocation" type—was somewhat easier to implement than QMOM, but preserves its generality with respect to PDF shape. In the present model problem (*n*-alkane vapors present in N_2 at 800 K and 1 atm) we have estimated significant Soret separation–induced dew-point shifts ($\sim$13 K), corresponding to incipient mixed-alkane condensate viscosity reductions of about 12%. We also illustrated the use of CMT combined with extended "mixing rules" to calculate the lower flammability limits (LFL) of such local hydrocarbon vapor mixtures in air.

These tractable CMT approaches to the formulation and solution of important multicomponent nonequilibrium thermodynamics problems, here illustrated for both cases, nearly thermodynamically "ideal" and "nonideal" condensates, appear to have considerable promise. Further applications/extensions (such as use of more than simply MW as a relevant state variable) to solve dynamical CMT problems of engineering importance are presently under active investigation.

Important generalizations of presently available work

Having gained valuable experience with the present CMT approaches to a canonical steady-state fluid-phase equilibrium problem, we are now in a position to investigate more complex fuel blend vaporization rate processes, including QS-droplet vaporization into a hot ambient environment. In a pioneering paper, Hallett[14] demonstrated the power of the simplest form of CMT applied to this problem, and his approach has recently been adopted/exploited in more complex simulations of multicomponent fuel spray behavior in turbulent mixing layers.[26] Based on the methods/results of the present paper, we are now in a position to systematically incorporate/study the effects of: (1) liquid-phase nonideality (either by UNIFAC or Wilson "local composition" model); (2) invoking our QMOM and SOC PDF simulation methods, which do not prescribe the functional form of the fuel concentration PDFs in vapor and liquid phases; (3) variability of species molecular diffusion coefficient (with carbon number); and (4) L-S (non-Fickian) fuel vapor mass transport.[10] Taking these enhancements in order:

(1) Although we do not anticipate large nonideality effects for fuel blends composed exclusively of *n*-alkanes, more accurate representations of real hydrocarbon fuels will have to take into account the simultaneous presence of aromatic and

branched-chain compounds, as well as alcohols. These constituents will increase the nonideality of such solutions, probably contributing to systematic distortions in the shape of the (multivariate?) concentration PDF in each phase.

(2) QMOM and SOC have been shown here, and in Arias-Zugasti and Rosner,[7] to be practical CMT methods to track univariate concentration PDFs in such multiphase transport/thermodynamic problems, including those governed by unsteady convective-diffusion balance equations (see, for example, Rosner[9] and Rosner et al.[27]). Both are capable of dealing with multivariate populations (see below), as will be necessary to deal with more complex fuel blends.

(3) The effective diffusion coefficients (and Soret) coefficients appearing in each of the selected moment evolution equations are systematically different, a variation that could be neglected in Hallett's quasi-constant property analysis.[14] In general, these systematic variations can be included in a straightforward manner.

(4) As emphasized in Rosner,[9] although most previous combustion calculations have explicitly considered nonunity Lewis number effects (that is, disparities between Fick diffusivities and thermal diffusivities), when these are important so is the Ludwig–Soret effect on fuel vapor mass transport (which has usually been neglected!). Indeed, gas kinetic theory reveals an interesting connection between the Soret factor and the fuel vapor Schmidt number,[10] so that the issue of "Lewis number effects in combustion" must be revisited from this perspective.

Future engineering applications; recommendations

As mentioned above, modeling more complex mixtures using the CMT approach will require suitable multivariate formulations. A practical step in this direction was taken by Willman and Teja,[28,29] who introduced the (admittedly nonorthogonal) choices: effective carbon number (by boiling point) and liquid-phase density. They exploited a five-moment method using prescribed lognormal-type PDFs in the coexisting phases to solve the canonical thermodynamic dew-point problem for a wide variety of complex mixtures (including natural gases, crude oils, and coal-derived liquids).

Our present methods (QMOM and SOC) appear to be capable of tracking the evolution of multivariate PDFs (see, for example, Rosner et al.[27] and Wright et al.[30]) in coexisting phases associated with fuel blend vaporization in spray devices, including combustors. We believe that this can be done using a more fundamentally attractive choice for the relevant state variables, and a demonstration of the success of this extended CMT approach for a canonical bivariate problem is the focus of our current work.

Acknowledgments

This work was supported, in part, by PRF (ACS) under Grant 40062-AC9, NSF under Grant 998 0747, HTCRE Lab Industrial Affiliates at Yale University, and UNED (Madrid) under project "Métodos Espectrales en Termodinámica de Mezclas Continuas." A portion of this article was presented as Paper 50b at the AIChE 2002 Annual Meeting (Indianapolis, IN). The authors are also pleased to acknowledge helpful discussions with Drs. R. McGraw, R. B. Diemer Jr., D. T. Wu, A. Gomez, M. Zurita-Gotor, Y. Khalil, R. Banki, and A. Firoozabadi.

Notation

$\langle C_p \rangle$ = molar heat capacity at constant pressure
H = Henry law constant
N = number of components in the mixture
N_Q = number of pseudo-components (abscissae) used in QMOM
$\hat{N}$ = number of pseudo-components (abscissae) used in SOC
n = number of carbon atoms in the n-alkane
$n_{\min}$ = number n of the lightest n-alkane of the mixture
$n_{\max}$ = number n of the heaviest n-alkane of the mixture
$\bar{n}$ = average carbon number in the mixture
M = number of groups in the mixture
M_n = molecular weight of the n-alkane CH
p = pressure level, MPa
Q_c = molar heat of combustion
Q = functional group *area* (UNIFAC)
q = pure component *area* (UNIFAC)
R = functional group *volume* (UNIFAC)
r = pure component *volume* (UNIFAC)
Sc = Schmidt number
T = absolute temperature, K
V = molar liquid volume
x = mole fraction in the liquid phase
y = mole fraction in the gas phase

Greek letters

α_T = thermal diffusion factor
Δn = average carbon number spread in the mixture
γ = activity coefficient
μ_L = condensate viscosity

Subscripts/superscripts

dp = dew point
∞ = in the bulk mainstream gas
G = in the gas phase
$i/j/k$ = pertaining to component/group $i/j/k$
L = in the liquid phase
mix = pertaining to the mixture
n = pertaining to the n-alkane C_nH_{2n+2}
w = at the condenser surface (V/L interface)

Abbreviations/acronyms

BL = boundary layer close to the surface of the condenser
CMT = continuous mixture theory
CVD = chemical vapor deposition
GQF = Gaussian quadrature formula
LFL = lower flammability limit
L-S = Ludwig–Soret
MOM = method of moments
MW = molecular weight
PDF = probability density function
QMOM = quadrature method of moments
SOC = spectral orthogonal collocation
UNIFAC = universal functional-group activity coefficients
VLE = vapor–liquid equilibrium
V/L = vapor/liquid

Literature Cited

1. Rosner DE. Thermal (Soret) diffusion effects on interfacial mass transport rates. *J Phys Chem Hydrodyn.* 1980;1:159-185.
2. Rosner DE, Nagarajan R. Transport-induced shifts in condensate dew-point and composition in multicomponent systems with chemical-reaction. *Chem Eng Sci.* 1985;40:177-186.
3. Rosner DE, Liang BS. Laboratory studies of the deposition of alkali sulfate vapors from combustion gases using a flash-evaporation technique. *Chem Eng Commun.* 1986;42:171-196.
4. Liang BS, Rosner DE. Laboratory studies of binary salt CVD in combustion gas environments. *AIChE J.* 1987;33:1937-1948.
5. Gal-Or B, Cullinan HT, Galli R. New thermodynamic-transport theory for systems with continuous component density distributions. *Chem Eng Sci.* 1975;30:1085-1092.
6. Cotterman RL, Prausnitz JM. Continuous thermodynamics for phase-

equilibrium calculations in chemical process design. In: Astarita G, Sandler SI, eds. *Kinetic and Thermodynamic Lumping of Multicomponent Mixtures*. Amsterdam: Elsevier; 1991:229-275.
7. Arias-Zugasti M, Rosner DE. Multicomponent fuel droplet vaporization and combustion using spectral theory for a continuous mixture. *Combust Flame.* 2003;135:271-284.
8. Rosner DE, Chen BK, Fryburg GC, Kohl FJ. Chemically frozen multicomponent boundary layer theory of salt and/or ash deposition rates from combustion gases. *Combust Sci Technol.* 1979;20:87-106.
9. Rosner DE. *Transport Processes in Chemically Reacting Flow Systems.* New York, NY: Dover; 2000.
10. Rosner DE, Israel RS, LaMantia B. Heavy species Ludwig–Soret transport effects in air-breathing combustion. *Combust Flame.* 2000; 123:547-560.
11. Poling BE, O'Connell J, Prausnitz J. *The Properties of Gases and Liquids.* 5th Edition. New York, NY: McGraw-Hill; 2000.
12. Rosner DE, Papadopoulos DH. Jump, slip, and creep boundary conditions at nonequilibrium gas/solid interfaces. *Ind Eng Chem Res.* 1996;35:3210-3222.
13. Vakili-Nezhaad GR, Modarress H, Mansoori GA. Continuous thermodynamics of petroleum fluids fractions. *Chem Eng Process.* 2001;40: 431-435.
14. Hallett WLH. A simple model for the vaporization of droplets with large numbers of components. *Combust Flame.* 2000;121:334-344.
15. National Institute of Standards and Technology (NIST). NIST Chemistry WebBook. Boulder, CO: NIST; 2003. Available at http://webbook.nist.gov/chemistry/
16. Yaws CL. *Chemical Properties Handbook.* New York, NY: McGraw-Hill; 1999.
17. Seider WD, Seader JD, Lewin DR. *Product and Process Design Principles: Synthesis, Analysis, and Evaluation* [cf. Eq. 1.2a, p. 28 Chap. 1]. Hoboken, NJ: Wiley; 2003.
18. Sandler SI. *Chemical and Engineering Thermodynamics.* 3rd Edition. New York, NY: Wiley; 1998.
19. Rosner DE, Günes D, Nazih-Anous N. Aerodynamically-driven condensate layer thickness distributions on isothermal cylindrical surfaces. *Chem Eng Commun.* 1983;24:275-287.
20. McGraw R. Description of aerosol dynamics by the quadrature method of moments. *Aerosol Sci Technol.* 1997;27:255-265.
21. Finlayson BA. *The Method of Weighted Residuals and Variational Principles. With Application in Fluid Mechanics, Heat and Mass Transfer.* New York, NY: Academic Press; 1972.
22. Gottlieb D, Orszag SA. *Numerical Analysis of Spectral Methods. Theory and Applications.* Philadelphia, PA: Society for Industrial and Applied Mathematics; 1977.
23. Villadsen J, Michelsen ML. *Solution of Differential Equation Models By Polynomial Approximation.* New York, NY: Prentice-Hall; 1978.
24. Canuto C, Hussaini MY, Quarteroni A, Zang TA. *Spectral Methods in Fluid Dynamics.* Berlin: Springer-Verlag; 1988.
25. Boyd JP. *Chebyshev and Fourier Spectral Methods.* 2nd Edition. New York, NY: Dover; 2000.
26. Le Clercq PC, Bellan J. Direct numerical simulation of a transitional temporal mixing layer laden with multicomponent-fuel evaporating drops using continuous thermodynamics. *Phys Fluids.* 2004;16:1884-1907. [See also paper 1G06, Proc of 30th Combustion Institute Symposium. Pittsburgh, PA: The Combustion Institute; 2004.]
27. Rosner DE, McGraw R, Tandon P. Multivariate population balances *via* moment and Monte Carlo simulation methods. *Ind Eng Chem Res.* 2003;42:2699-2711.
28. Willman BT, Teja AS. Continuous thermodynamics of phase equilibria using a multi-variate distribution function and an equation of state. *AIChE J.* 1986;32:2067-2078.
29. Willman BT, Teja AS. Prediction of dew points of semicontinuous natural-gas and petroleum mixtures. 2. Nonideal solution calculations. *Ind Eng Chem Res.* 1987;26:953-957.
30. Wright R, McGraw R, Rosner DE. Bivariate extension of the quadrature method of moments for modeling simultaneous coagulation and sintering of particle populations. *J Colloid Interface Sci.* 2001;236: 242-251.

Manuscript received Sep. 7, 2004, and revision received Jan. 18, 2005.